

The Influence of Structure on the Physico-chemical Properties of Slags

Kenneth C. MILLS

Division of Materials Metrology, National Physical Laboratory, Teddington, Middx, TW 11 OLW, UK.

(Received on May 18, 1992; accepted in final form on September 18, 1992)

The current knowledge of the structures of silicate slags is summarised and the relationships between measures of the depolymerisation of the melt and various physical properties are examined. It is shown that the optical basicity when corrected for the cations required to charge-balance any AlO_4^{5-} tetrahedra present, provides a reasonable measure of the depolymerisation of the melt and has the advantage over the (NBO/T) ratio that it compensates for cation effects. It is shown that the depolymerisation of the melt is the primary factor affecting most physical properties, the cations having only a secondary effect. The relationships between structure and the viscosity, electrical and thermal conductivity, diffusion coefficient, density, thermal expansion coefficient, thermodynamic and optical properties of melts are discussed.

KEY WORDS: slags; structure; viscosity; electrical conductivity; thermal conductivity; diffusion coefficient; thermal expansion coefficient; optical basicity; (NBO/T).

1. Introduction

In the last decade the mathematical modelling of high temperature processes has become an established method for improving the performance and efficiency of these processes. Mathematical modelling of the heat and fluid flow in these processes has resulted in a demand for physical property data for the materials involved. The determination of reliable physical property data at high temperature is both difficult and time-consuming. Furthermore, the compositions of slag phases formed in high temperature processes may differ significantly from day-to-day and also plant engineers frequently wish to know the effect that changing the concentrations of certain constituents of the slag would have on the performance of the process. All of these factors have led to a demand for mathematical models to predict the physical properties as a function of the chemical composition.

Various models have been reported for the prediction of liquidus temperature, T_{liq} ^{1,2)} viscosity,³⁻⁵⁾ density^{6,7)} etc. of the slag phase. These models for the most part are based on numerical fits of experimental data and are rarely based on the structure of slag. However, the dependence of the physical properties upon the structure of silicate melts is demonstrated by the fact that Bockris^{8,9)} and other workers were able to deduce the structure from physical property measurements. Thus the demand for more reliable estimates of the physical properties of slags will only be met by the development of models based on the structure of the slag.

Our knowledge of slag structure has improved enormously in recent years with the introduction of new

techniques such as X-ray and neutron diffraction,¹⁰⁾ vibrational (especially Raman) spectroscopy and nuclear magnetic resonance. Data from these sources combined with information from structural thermodynamic models, molecular dynamics calculations and physical property data has led to a rapid advance in our knowledge of the structure of silicates. Many of these advances have come from the studies of the structures of magmas and rocks by the geological fraternity. The current status of our knowledge of the silicate melts has been described by Mysen¹¹⁾ in two excellent reviews.

The structures of silicate melts are affected by (1) the degree of polymerisation of the silicate melt (2) the fitting of certain cations (eg. Al^{3+} , Ti^{4+}) into the silicate network and (3) the nature of the network-breaking cations (eg. Ca^{2+} , Mg^{2+}) present in the slag. The aim of the present study was to identify their effects on the physical properties of the molten slag.

2. Structure of Silicates

The principal features affecting the structure of molten silicates¹¹⁾ are outlined below:

(1) Silicate slags consist of 3-dimensional (3-D) interconnected networks of SiO_4^{4-} tetrahedra in which silicons are joined by bonding oxygen atoms (O°). The gradual addition of cations (eg. Na^+ , Ca^{2+}) results in the progressive breaking of these oxygen bonds with the formation of non-bridging oxygens (NBO), denoted O^- and eventually the formation of free oxygen, O^{2-} , ions.

(2) The melt contains various 3-D interconnected, anionic units, eg. SiO_2 , $\text{Si}_2\text{O}_5^{2-}$, $\text{Si}_2\text{O}_6^{4-}$, $\text{Si}_2\text{O}_7^{6-}$ and SiO_4^{4-} which coexist in the melt. These anionic units

probably contain 3–6 atoms and can exist in the form of chains, sheets and rings. The introduction of more network-breaking cations, *eg.* Ca^{2+} does not alter the nature of the anionic units but does affect the amounts of the various units, *i.e.* high concentrations of more depolymerised units are formed.

(3) For a specific mole fraction (x) of oxide (*eg.* $x(\text{CaO})$) the nature of the cation does affect the proportion of the various units, *eg.* $\text{Si}_2\text{O}_7^{6-}$ but not the overall degree of polymerisation. The cations with smaller radii (r) and higher valence (z), *eg.* Mg^{2+} , favour the formation of the more depolymerised (*eg.* SiO_4^{4-}) and polymerised (*eg.* SiO_2) anionic units. The tendency to form more extreme anionic units can be ranked in terms of the parameter (z/r^2) in the hierarchy $\text{Mg}^{2+} > \text{Ca}^{2+} > \text{Sr}^{2+} > \text{Pb}^{2+} > \text{Ba}^{2+} > \text{Li}^+ > \text{Na}^+ > \text{K}^+$.

(4) Other cations such as Al^{3+} , Fe^{3+} , B^{3+} , Ti^{4+} and P^{5+} can form tetrahedra (*eg.* AlO_4^{5-}) which usually fit into the 3-D silicate units and enhance the overall polymerisation of the melt; thus it is customary to refer to tetrahedrally-coordinated units by T rather than Si, *eg.* TO_2 , T_2O_5 *etc.* However, AlO_3^{3-} ions have a different charge to SiO_4^{4-} tetrahedra, and thus cations are needed, to provide electrical charge balance, *eg.* $(\text{NaAlO}_4)^{4-}$ and thus the Na^+ must be sited close to the Al atom.

(5) There is some evidence of ordering in melts containing divalent ions (*eg.* Ca^{2+}) since these must satisfy two O^- bonds or two AlO_4^{5-} tetrahedra and this task is particularly difficult for smaller cations, *eg.* Mg^{2+} , and hence the need for ordering of the melt.

(6) Ferric ions, Fe^{3+} can adopt both four-fold (IV) or six-fold (VI) coordination, *i.e.* act as both network former and breaker, respectively. For slags containing 10% Fe_2O_3 it has been reported^{11,12)} that Fe^{3+} (IV) and (VI) coordination are favoured when the $\text{Fe}^{3+}/(\text{Fe}^{3+} + \text{Fe}^{2+})$ ratios are >0.5 and <0.3 , respectively. In most steelmaking slags Fe^{3+} will act as a network-breaker (VI).

(7) In aluminosilicates the Al probably prefers the more polymerised units (*eg.* TO_2) of with a large T–O–T angle.

(8) Ti can also adopt IV and VI coordination, it is reported¹¹⁾ that for 1–7 mass% TiO_2 the Ti acts as network former but the substitution is not random and tends to form titanates and aluminotitanates.

(9) P_2O_5 tends to form PO_4^{3-} tetrahedra but although some P–O–Si bonds are formed, the P_2O_5 tends to form phosphate complexes which have a greater affinity for cations, *eg.* Na^+ , Al^{3+} than SiO_4^{4-} tetrahedra.

2.1. Measures of the Degree of Polymerisation

In recent years the (NBO/T) ratio, *i.e.* the number of non-bridging oxygens per tetrahedrally-coordinated atom, has been adopted by many workers to represent the degree of depolymerisation of the melt. It can be seen from Appendix 1 that the (NBO/T) ratio does allow for the cations occupied on charge-balancing duties. The (NBO/T) ratio is probably the best measure of the degree of polymerisation.

Considerable attention has been devoted recently to

the optical basicity (A) which represents the power of an oxide to donate a negative charge. However the optical basicity has been reported to provide a global measure of the concentrations of O^0 , O^- and O^{2-} present in the melt.¹³⁾ Consequently, the optical basicity may be considered to provide an alternative measure of the degree of polymerisation. However the optical basicity (A) does not take into account the fact that some of the cations in aluminosilicates are required for charge balancing duties; hence an adjustment was made to A (outlined in Appendix 2) to compensate for the cations used for charge balancing. The principal advantage of using A_{corr} is that it can be applied to non-silicate slags.

2.2. Cation Effect

Various parameters have been used as a measure of the effect of different cations on the structure and physical properties; Mysen¹¹⁾ preferred the parameter (z/r^2) where z and r are the valence and radius of the cation, respectively. It can be seen from Fig. 1 that (z/r^2) is inversely proportional to the optical basicity of the oxide.

3. Physical Properties

Most physical properties are strongly dependent upon temperature, thus when comparing slags with different liquidus temperatures, T_{liq} , it is necessary to compare property values at some reference temperature. The value at T_{liq} was selected since the structures of the melt would be unaffected by temperature effects and would allow the physical properties to be compared on an equal basis.

The temperature dependence of most transport properties can be represented by the Arrhenius relationship (Eq. (1)) where P is the property, E the activation energy, R the gas constant and T the thermodynamic temperature.

$$P = A \exp(-E_p/RT) = A \exp(-B_p/T) \dots\dots\dots(1)$$

The activation energy for viscous flow is considered to be the energy required to break the bonds necessary for viscous flow, consequently the activation energy could also be used to determine the effect of structure on physical properties.

3.1. Viscosity (η)

Viscosity (η) data are prone to appreciable errors, a recent interlaboratory comparison programme indicated that some of the reported viscosities for a reference material varied by more than $\pm 50\%$ from the

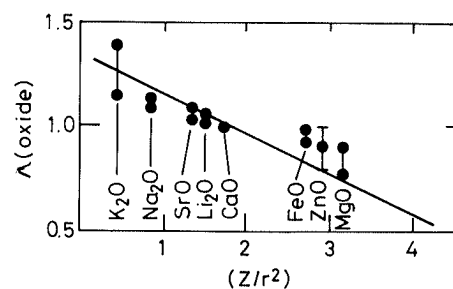


Fig. 1. The parameters (z/r^2) as a function of the optical basicity, A .

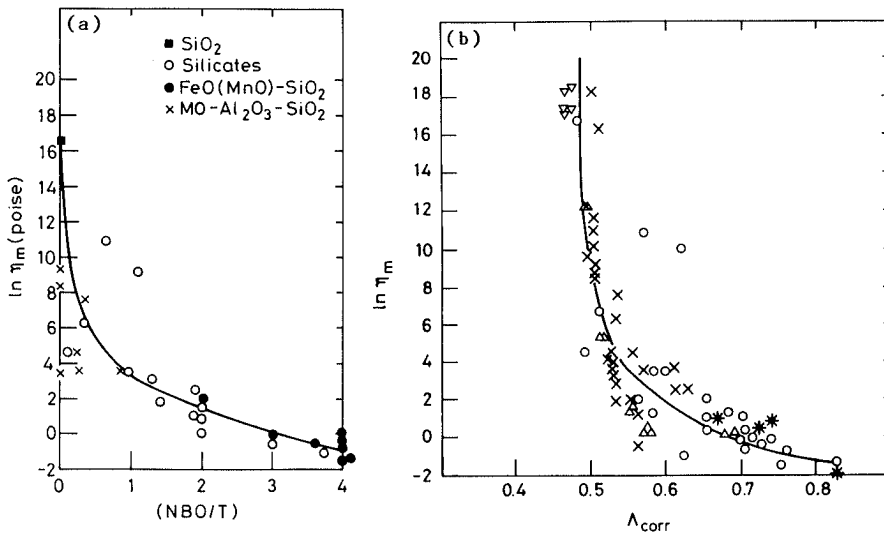


Fig. 2. The viscosity at the liquidus temperature ($\ln \eta_m$) as a function of (a) (NBO/T) ratio and (b) corrected optical basicity, Λ_{corr} . \circ , \bullet , silicates, \times , aluminosilicates. *: calcium aluminates, Δ : $\text{SiO}_2\text{-Al}_2\text{O}_3$, ∇ : $\text{SiO}_2\text{-B}_2\text{O}_3$.

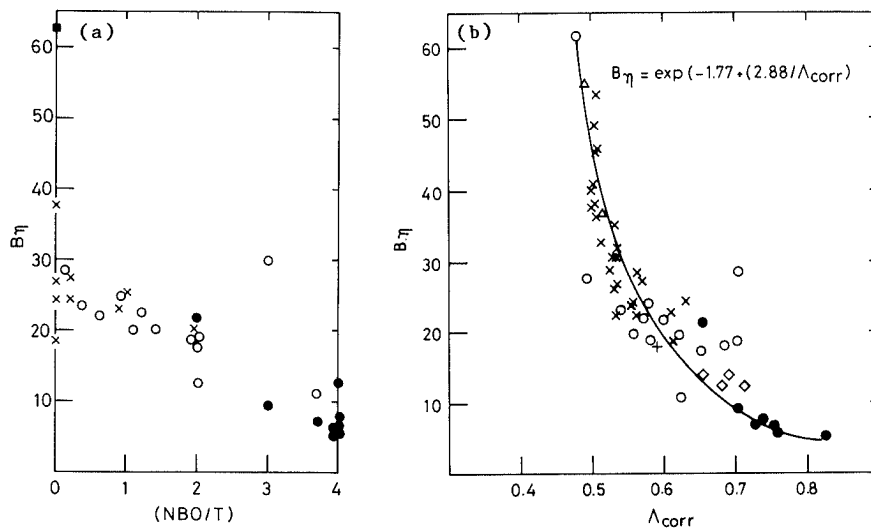


Fig. 3. The parameters, B_η ($=E_\eta/R$) as a function of (a) the (NBO/T) ratio and (b) the corrected optical basicity, Λ_{corr} . \circ , \bullet , silicates, \times , $+$: aluminosilicates, \diamond : systems containing Fe_2O_3 , Δ : $\text{SiO}_2\text{-Al}_2\text{O}_3$.

recommended values.*¹⁴⁾ In order to eliminate the systematic differences in the viscosity associated with differences in experimental procedure used by different laboratories, it was decided to use only the data reported by Urbain *et al.*¹⁵⁻¹⁸⁾ since these data should be self consistent and should reveal any trends due to depolymerization, cation effects *etc.* It was also noted that viscosity values recorded by Urbain *et al.*¹⁵⁻¹⁸⁾ for various reference materials for high temperature viscosity measurements were in good agreement with the recommended values.

The relationships between $\ln \eta_m$ and the (NBO/T) ratio and Λ_{corr} are shown in **Figs. 2(a)** and **2(b)** respectively. The following observations were made:

(1) The two divergent points in **Figs. 2(a)** and **2(b)** were for two $\text{Na}_2\text{O-SiO}_2$ slags with very low T_{liq} , the deviations could be due to the long extrapolations required.

(2) It can be seen from **Fig. 2(a)** that there are appreciable differences in the $\ln \eta_m$ values for the aluminosilicates with (NBO/T)=0 and the deviation was found to increase with increasing Al content. Inspection

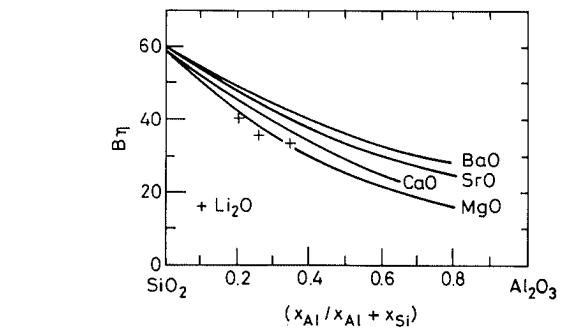


Fig. 4. The effect of Al substitution of Si in the silicate network upon the activation energy parameter, B_η .

of **Fig. 2(b)** indicates the Λ_{corr} provides some compensation for the effect of Al_2O_3 on $\ln \eta_m$.

Values of B_η ($=E_\eta/R$) are plotted as functions of (NBO/T) and Λ_{corr} in **Figs. 3(a)** and **3(b)** respectively. It can be seen that in **Fig. 3(a)** that B_η values for aluminosilicates with (NBO/T)=0 showed considerable scatter. The effects of Al substitution of the Si on B_η are shown in **Fig. 4**. This behaviour results mainly from the

* Based on the mean of five determinations lying within a scatterband of $\pm 10\%$.

fact that the bond length of Al-O is longer than that of Si-O (1.715 cf. 1.58 Å).¹¹⁾

It can be seen from Fig. 3(b) that A_{corr} allows some compensation for the effect of Al_2O_3 on B_η . It can also be observed in Fig. 4 that the effect of Al_2O_3 on B_η increases as (z/r^2) for the cation increases (or A for the oxide decreases). This may be a consequence of increased ordering produced when small, divalent cations are needed to charge balance two AlO_4^{5-} tetrahedra.

The pre-exponential term A_η is shown as function of A_{corr} in Fig. 5. One of the attractions of the optical basicity concept is that it could be applied to other forms of slags and it can be seen from Fig. 6 that the relationships for borates and phosphates have a similar form to that of silicates but the curves are moved to lower optical basicities since $A(\text{B}_2\text{O}_3)$ and $A(\text{P}_2\text{O}_5)$ are lower than $A(\text{SiO}_2)$. Recent work¹⁹⁾ has shown that viscosities of glasses for temperatures between T_{liq} and the glass transition temperature (T_g) can be reliably estimated using A_{corr} .

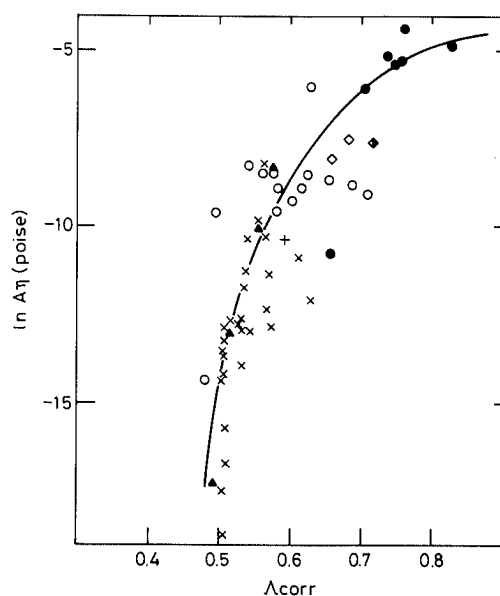


Fig. 5. The Arrhenius pre-exponential term, A_η , as a function of the corrected optical basicity; ○, ●; silicates, ×, +: aluminosilicates, ◇, ◊; systems containing Fe_2O_3 .

3.2. Electrical Conductivity (κ)

Specific electrical conductivity (κ) data reported by Bockris *et al.*^{20,21)} for 8 binary silicate systems were extrapolated to T_{liq} and values for aluminosilicates were those reported by Winterhager *et al.*²²⁾ Bockris *et al.* noted that the activation energy E_κ (unlike E_η) did not vary much with SiO_2 content and suggested that the mobility of the cations (*e.g.* Ca^{2+}) was the most important mechanism affecting electrical conduction. Thus higher electrical conductivities might be expected for systems with (1) cations with high values of (z/r^2) or low A values and (2) more depolymerised melts, *i.e.* high (NBO/T) and A_{corr} values.

Plots of $\ln \kappa_m$ as a function of (NBO/T) and A_{corr} are shown in Figs. 7(a) and 7(b), respectively, and the following observations were made:

(1) The values of $\ln \kappa_m$ increases markedly with increasing depolymerisation, *i.e.* increasing NBO/T and A_{corr} values, and thus it appears that the hindrance of cationic mobility by the silicate network is the primary factor affecting electrical conductivity, especially in the acidic region.

(2) The $\ln \kappa_m$ values for Group I oxides were higher

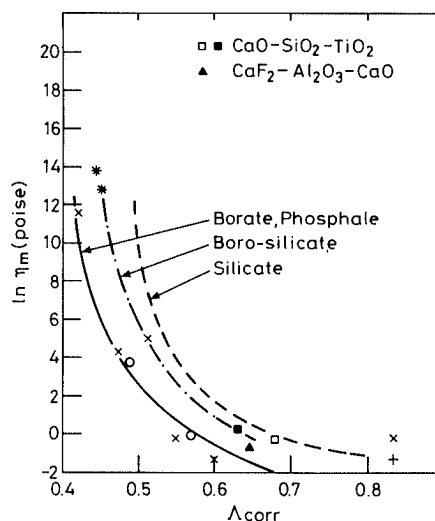


Fig. 6. The $\ln \eta_m$ for borates and phosphates as function of A_{corr} , ×, borates, *: borosilicates, ○, phosphates, +: $\text{CaO-Al}_2\text{O}_3$.

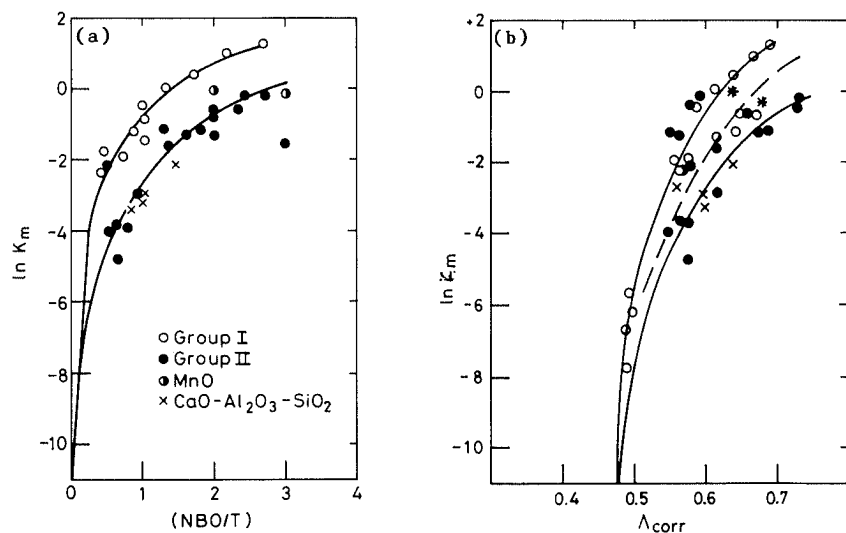


Fig. 7. The electrical conductivity at T_{liq} ($\ln \kappa_m$) as functions of (a) (NBO/T) and (b) the corrected optical basicity.

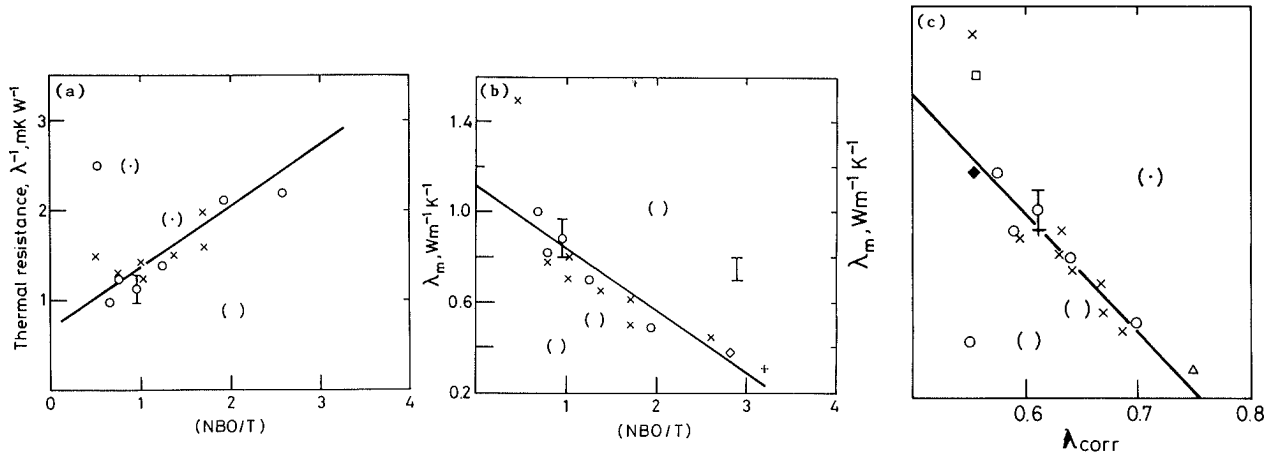


Fig. 8. The effect of (NBO/T) on the (a) thermal resistance and (b) thermal conductivity and (c) shows the latter as a function of λ_{corr} .

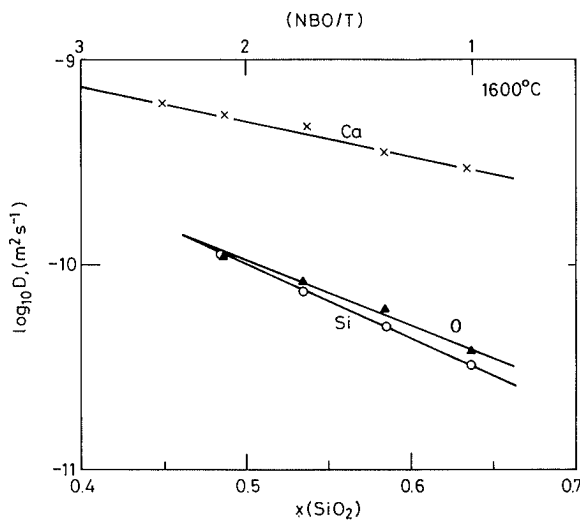


Fig. 9. The self diffusion coefficients, D of Ca, Si and O at 1600°C as a function of mole fraction SiO_2 and (NBO/T).²¹⁻²⁹⁾

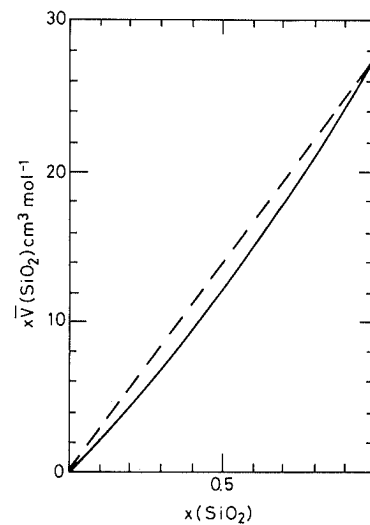


Fig. 10. The parameter, $x\bar{V}(\text{SiO}_2)$, as a function of both mole fraction SiO_2 and (NBO/T).

than those for Group II oxides; this may be due to ordering of the melt to accommodate the need for M^{2+} ions to be sited near two O^- .

(3) Although $\ln \kappa_m$ values decreased in the hierarchy $\text{Li}_2\text{O} > \text{Na}_2\text{O} > \text{K}_2\text{O}$ and $\text{MgO} > \text{CaO} > (\text{SrO}, \text{BaO})$, *i.e.* increasing cationic radius, however the differences were small.

(4) Since $\ln \kappa_m$ values for the aluminosilicates are in agreement with those for silicates with similar (NBO/T) or λ_{corr} , it was concluded that the cations involved in charge balancing duties do not contribute to the electrical conductivity of the melt.

On the basis of these observations it was concluded that degree of depolymerisation was the primary factor affecting the electrical conductivity of the melt, especially for SiO_2 -rich compositions.

3.3. Thermal Conductivity (λ)

Accurate values of the thermal conductivities of melts are notoriously difficult to obtain since the measured values can contain large contributions from both convection and radiation conduction. In order to

minimise these contributions transient techniques have been used, the values at T_{liq} obtained using these methods have been employed here.²³⁻²⁷⁾

It has been suggested²⁸⁾ that the thermal resistance ($1/\lambda$) associated with the movement of phonons along the silicate chain or ring is relatively small when compared with that associated with the movement of phonons from chain to chain. Thus the thermal resistance ($1/\lambda$) would be expected to increase as the melt becomes progressively depolymerised. It can be seen from Fig. 8 that the experimental data are in agreement with this proposition. Consequently it might be expected that melts with large cations would have higher conductivities, unfortunately, there are insufficient data to deduce whether the size of the cation has any effect on the thermal conductivity of the melt.

3.4. Self Diffusion Coefficients (D)

Experimental data for self diffusion coefficients, D , in liquid slags are prone to large experimental uncertainties. Nevertheless, the effect of the degree of depolymerisation of the melt on the diffusion coefficient can be clearly seen in the results obtained for the CaO-SiO_2 system²⁹⁻³¹⁾

shown in Fig. 9.

The experimental uncertainties in the $D(\text{Ca})$ values for the $\text{CaO-Al}_2\text{O}_3\text{-SiO}_2$ system were considered to be too large to determine whether the cations on charge-balancing duties play a part in the diffusion processes.

3.5. Molar Volume (V) Density (ρ)

Molar volumes (V) for mixed oxides can usually be estimated accurately using Eq. (2) where x is the mole fraction and \bar{V} is the partial molar volume of the oxide and usually has a fixed value.⁷⁾

$$V = x_1 \bar{V}_1 + x_2 \bar{V}_2 + x_3 \bar{V}_3 + \dots \dots \dots (2)$$

The values for $x_1 \bar{V}_1$ for SiO_2 can be obtained from experimental molar volume data for slags (using Eq. (3))

$$x_1 \bar{V}_1 = V - x_2 \bar{V}_2 - x_3 \bar{V}_3 \dots \dots \dots (3)$$

It can be seen from Fig. 10 that there is a small departure from linearity which presumably is a result of structural effects.

3.6. Thermal Expansion Coefficients ($\bar{\alpha}$)

Thermal expansion coefficients ($\bar{\alpha}$) data for the liquids^{21,32,33)} have been shown to be functions of (NBO/T) and Λ_{corr} in Figs. 11(a) and 11(b). The thermal

expansion coefficients can be seen to increase as:

- (1) the melt becomes more depolymerised, *i.e.* (NBO/T) and Λ_{corr} increase;
- (2) the parameter (z/r^2) decreases for the cation or $\Lambda(\text{MO})$ increases.

It can also be seen that $\bar{\alpha}$ values for the aluminosilicates agree well with the values for silicates with equivalent (NBO/T) or Λ_{corr} and that the use of Λ_{corr} compensates for the effect of cation size and charge.

3.7. Surface Tension (γ)

Although the surface tension (γ) of a slag is not a bulk property like those discussed above, there are indications that the surface properties may be affected by the structure of the liquid. Positive temperature coefficients ($d\gamma/dT$) has been reported^{34,35)} in slags with high SiO_2 contents and this behaviour may be associated with the presence of BO's on the surface.

3.8. Thermodynamic Properties

Our current knowledge of the structure of silicates has been assisted by the development of mathematical models to calculate thermodynamic properties of silicate systems^{1,2,37)} and some of these models provide estimates of the number of tetrahedrally coordinated Si atoms in

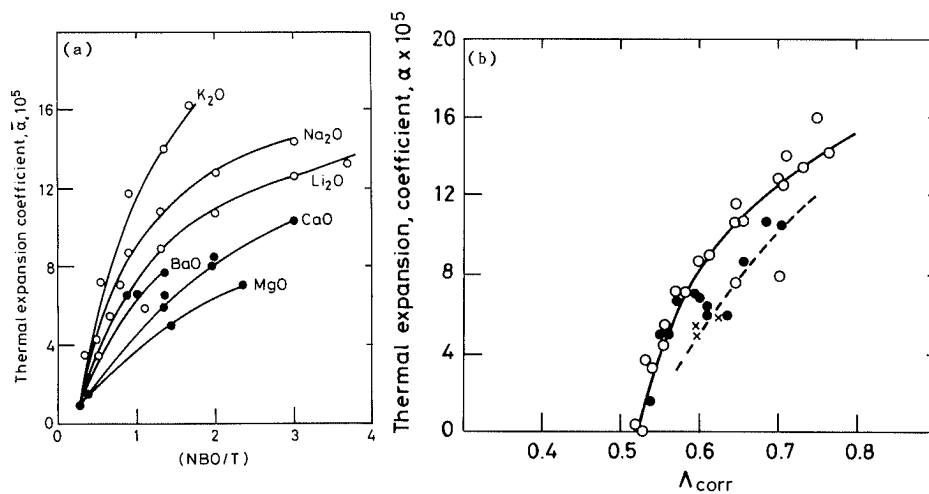


Fig. 11. Thermal expansion coefficients ($\bar{\alpha}$) as a function of (a) (NBO/T) and (b) the corrected optical basicity; \circ , \bullet , silicates, \times , aluminosilicates.

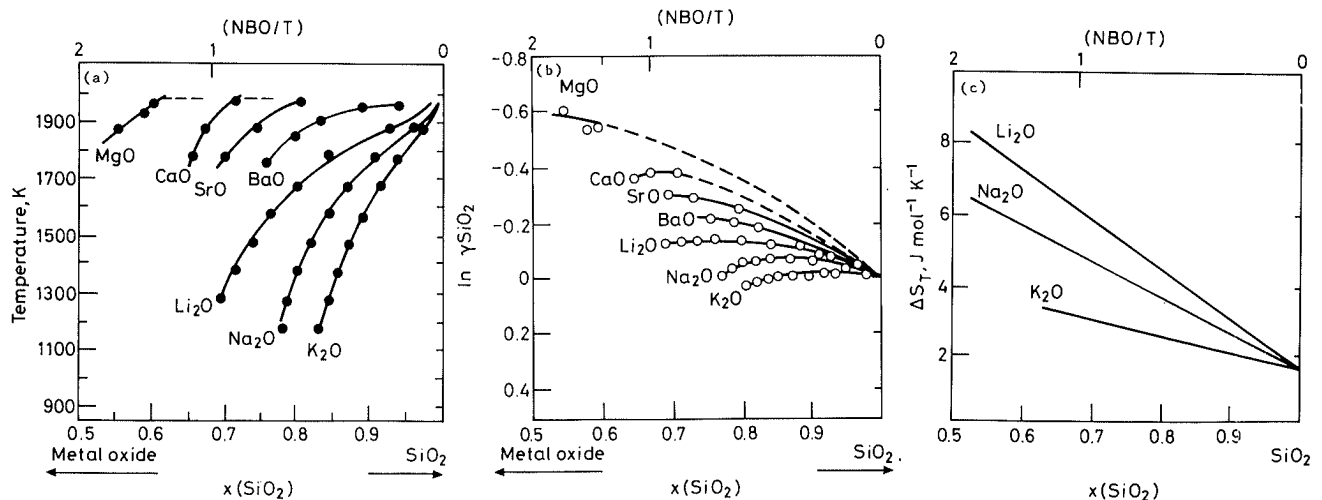


Fig. 12. (a) Liquidus temperature, (b) activity coefficient of SiO_2 and (c) entropy of fusion as a function of mole fraction SiO_2 and (NBO/T) ratio.

the chain or ring.^{36,37} However the effect of the degree of polymerisation on thermodynamic properties can be clearly be seen in Fig. 12, *i.e.* that (1) the T_{liq} values increase with decreasing (NBO/T) ratios in the range 0 to 2, (2) the depression in T_{liq} is greater for Group I oxides than for Group II oxides and (3) within any one Group the depression increases with decreasing (z/r^2) for the cation (or increasing A for the oxide).

These same trends are shown in Figs. 12(b) and 12(c) where the activity coefficient of SiO_2 and the entropy of fusion are shown as function of $x(SiO_2)$ and NBO/T. The cation effects may be due to the ordering of the melt required to enable divalent cations to be sited near two O^- ions.

3.9. Optical Properties

The addition of network-breaking cations to the SiO_2 network results in the destruction of O° bonds and the formation of O^- and O^{2-} . Under these circumstances the electron polarisability of the oxygen is increased and this results in an increase in refractive index.³⁸ In fact refractive index measurements have been used by Iwamoto *et al.*³⁸ to determine the relative amounts of O° , O^- and O^{2-} . There is also evidence to show that the absorption edge in visible/ultra-violet region (associated with the charge transfer band) is moved to higher wavelengths as a result of increased electron polarisation.³⁹

3.10. Sulphur and Phosphorus Capacities

Optical basicities have been used by several investigators to calculate the sulphur and phosphorus capacities of slags. Recently the corrected optical basicity has been correlated with sulphur capacity data derived from many sources.³⁹ It was found that there was considerably less scatter in these plots than with those obtained using the uncorrected optical basicity. However the use of A_{corr} had little effect on the P capacity correlation which could only be improved by using a much smaller value of $A(FeO)$.⁴⁰

4. Future Work

The relationships of individual physical properties with global measures of the degree of polymerisation, *i.e.* (NBO/T) and A_{corr} , will lead to development of improved mathematical models for the estimation of physical properties of slags. However, Mysen¹¹ has shown that it is possible to calculate the relative concentrations of various anionic units. Correlations between physical properties and the concentration of anionic units, *eg.* T_2O_5 could be used to develop predictive models and these could lead to improved accuracy in the predicted values. However, before this approach can be applied rigorously to multicomponent industrial slags further information will be needed on the way that elements such as P, and Ti influence the relative concentrations of the anionic units like TO_2 , T_2O_5 *etc.*

5. Conclusions

- (1) The degree of depolymerisation of the melt is the

primary factor affecting most physical properties; the effect of different cations tends to be "second order" for most of the properties studied.

- (2) Although the (NBO/T) ratio is probably superior to A_{corr} as a measure of the depolymerisation of silicate melts, the latter has the advantages that it is capable of application to non-silicate systems and makes some compensation for the effect of the cations.

- (3) For alumino-silicates, it would appear that cations involved in charge-balancing duties do not contribute to the depolymerisation of the melt.

- (4) The (NBO/T) ratio can not account for the effect of the longer Al-O bond lengths on the activation energy for viscous flow in alumino-silicates, whereas A_{corr} provides some compensation.

- (5) There is some evidence of "ordering" in melts containing small, divalent cations such as Mg^{2+} . This ordering may result from the need for the Mg^{2+} cations to be sited near two O^- or two AlO_4^{5-} tetrahedra.

Acknowledgements

The useful discussions held with Brian Keene, Paul Grieveson, Åke Bergman, Bob Young (British Steel) and Masahiro Susa are gratefully acknowledged. This work was carried out for the "Materials Measurement Programme" financed by the UK, Department of Trade and Industry.

REFERENCES

- 1) H. Gaye and J. Welfringer: Proc. of 2nd Int. Symp. on Metallurgical Slags and Fluxes, Lake Tahoe, Nevada, (1984).
- 2) A. D. Pelton and M. Blander: Proc. of 2nd Int. Symp. on Metallurgical Slags and Fluxes, Lake Tahoe, Nevada, (1984), 281.
- 3) P. V. Riboud, Y. Roux, L. D. Lucas and H. Gaye: *Fachber. Hüttenprax. Metallweiter verarb.*, **19** (1981), 859.
- 4) W. D. McCauley and D. Apelian: *Can. Metall. Q.*, **20** (1981), 247.
- 5) G. Urbain: *Steel Res.*, **58** (1987), 111.
- 6) H. Bottinga and D. E. Weill: *Amer. J. Sci.*, **272** (1972), 438.
- 7) K. C. Mills: Mineral Matter and Ash in Coal, Vol. 301, Amer. Chem. Soc. Monographic Series, (1986), 197.
- 8) J. O'M. Bockris, J. D. Mackenzie and J. A. Kitchener: *Trans. Farad. Soc.*, **51** (1954), 1734.
- 9) J. O'M. Bockris and A. K. N. Reddy: Modern Electrochemistry, Plenum Press, New York, (1970).
- 10) Y. Waseda and J. M. Toguri: *Metall. Trans. B.*, **8B** (1977), 563.
- 11) B. O. Mysen: Structure and Properties of Silicate Melts, Elsevier, Amsterdam, (1988); B. O. Mysen: *Earth Science Rev.*, **27** (1990), 281.
- 12) K. Morinaga, Y. Sugihara and T. Yanagase, *J. Jpn. Inst. Met.*, **40** (1976), 480 and 775.
- 13) J. A. Duffy: *Iron Steelmaking*, **17** (1990), 410.
- 14) K. C. Mills: NPL Report DMM(A)30, (1991), available from National Physical Laboratory, Teddington, Middlesex, UK.
- 15) G. Urbain, Y. Bottinga and P. Richet: *Geochim. Cosmochim. Acta*, **46** (1982), 1061.
- 16) G. Urbain: *Rev. Int. Haut. Temp. Réfract.*, **22** (1986), 39.
- 17) G. Urbain: *Rev. Int. Haut. Temp. Réfract.*, **20** (1983) 135.
- 18) G. Urbain, F. Millon and S. Cariset: *CR Acad. Sci. Paris*, **290** (1980), 137.
- 19) F. Y. Yan, F. W. Wood and K. C. Mills: Proc. of XV Int. Glass Congress, Vol. 2, Madrid, Oct., (1992), 177.
- 20) J. O'M. Bockris, J. A. Kitchener, S. Ignatowicz and J. W. Tomlinson: *Faraday Soc. Discuss.*, **6** (1948), 265.
- 21) J. O'M. Bockris, J. A. Kitchener, S. Ignatowicz and J. W. Tomlinson: *Trans. Faraday Soc.*, **48** (1952), 75.
- 22) H. Winterhager, L. Geiner and R. Kammel: Forschungber des Landes Nordrhein-Westfalen, 1630 Köln/Opladen, (1966).

- 23) T. Sakuraya, T. Emi, H. Ohta and Y. Waseda: *J. Jpn. Inst. Met.*, **46** (1982), 1131.
- 24) M. Kishimoto, M. Maeda, K. Mori and Y. Kawai: Proc. 2nd Int. Symp. on Metallurgical Slags and Fluxes, ed. by H. A. Fine and D. R. Gaskell, Metall. Soc. AIME, Warrendale, PA, (1984), 891.
- 25) H. Ohta, Y. Waseda and Y. Shiraishi: Proc. 2nd Int. Symp. on Metallurgical Slags and Fluxes, ed. by H. A. Fine and D. R. Gaskell, Metall. Soc. AIME, Warrendale, PA, (1984), 863.
- 26) K. Nagata and K. S. Goto: Proc. 2nd Int. Symp. on Metallurgical Slags and Fluxes, ed. by H. A. Fine and D. R. Gaskell, Metall. Soc. AIME, Warrendale, PA, (1984), 875.
- 27) F. Li, M. Susa and K. Nagata: *J. Jpn. Inst. Met.*, **55** (1991), 194.
- 28) K. C. Mills: Proc. 3rd Int. Conf. on Metall. Slags and Fluxes, Inst. of Met., London, (1989) 229.
- 29) H. Keller, K. Schwerdtfeger and K. Hennesen: *Metall. Trans. B*, **10B** (1979), 67.
- 30) H. Keller and K. Schwerdtfeger: *Metall. Trans. B*, **10B** (1979), 551.
- 31) H. Keller, K. Schwerdtfeger, H. Petri, R. Holzle, K. Hennesen: *Metall. Trans. B*, **13B** (1982), 237.
- 32) J. O'M. Bockris, J. D. MacKenzie and J. A. Kitchener: *Trans. Faraday Soc.*, **51** (1955), 1734.
- 33) J. W. Tomlinson, M. S. R. Haynes, J. O'M. Bockris: *Trans. Faraday Soc.*, **54** (1958), 1822.
- 34) T. B. King: *J. Soc. Glass Technol.*, **35** (1951), 241.
- 35) K. C. Mills, B. J. Keene: *Int. Mater. Rev.*, **32** (1987), 1.
- 36) P. L. Lin and A. D. Pelton: *Metall. Trans. B*, **10B** (1979), 667.
- 37) C. Borgianni and P. Granati: *Metall. Trans. B*, **10B** (1979), 21.
- 38) N. Iwamoto and Y. Makino: *J. Non-Cryst. Solids*, **34** (1979), 381.
- 39) M. Susa, F. Li and K. Nagata: *Metall. Trans. B*, **23B** (1992), 331.
- 40) R. Young: Private communication, British Steel Teesside Laboratories, Grangetown, Middlesbrough, UK., April, (1992).

Appendix 1

Calculation of NBO/T

$$\begin{aligned}
 Y_{\text{NB}} &= \sum 2[x(\text{CaO}) + x(\text{MgO}) + x(\text{FeO}) \\
 &\quad + x(\text{MnO}) + x(\text{Na}_2\text{O}) + x(\text{K}_2\text{O})] \\
 &\quad + 6(1-f)x(\text{Fe}_2\text{O}_3) - 2x(\text{Al}_2\text{O}_3) \\
 &\quad - 2fx(\text{Fe}_2\text{O}_3) \\
 x_T &= \sum x(\text{SiO}_2) + 2x(\text{Al}_2\text{O}_3) + 2fx(\text{Fe}_2\text{O}_3) \\
 &\quad + x(\text{TiO}_2) + 2x(\text{P}_2\text{O}_5)
 \end{aligned}$$

$$(\text{NBO}/T) = (Y_{\text{NB}}/x_T)$$

where x = mole fraction,

$$f = \text{Fe}^{3+}(\text{IV}) / (\text{Fe}^{3+}(\text{IV}) + \text{Fe}^{3+}(\text{VI})),$$

i.e. fraction of Fe^{3+} with IV coordination.

Appendix 2

Calculation of Optical Basicity

$$A = \frac{\sum x_1 n_1 A_1 + x_2 n_2 A_2 + x_3 n_3 A_3 + \dots}{\sum x_1 n_1 + x_2 n_2 + x_3 n_3 + \dots}$$

where n is the number of oxygens in the oxide, eg. 3 for Al_2O_3 , 2 for SiO_2 .

Values of A_{th} used in the calculation of A

K ₂ O	Na ₂ O	BaO	SrO	Li ₂ O	CaO	MgO	Al ₂ O ₃
1.4	1.15	1.15	1.10	1.0	1.0	0.78	0.60
TiO ₂	SiO ₂	B ₂ O ₃	P ₂ O ₅	FeO	Fe ₂ O ₃	MnO	CaF ₂
0.61	0.48	0.42	0.40	1.0	0.75	1.0	0.43

Calculation of A_{corr}

Take a slag of composition, (0.5SiO₂+0.15Al₂O₃+0.2CaO+0.1MgO+0.05K₂O), the AlO₄⁵⁻ are charge balanced by cations with higher A values: thus K₂O > CaO > MgO. Thus 0.15(oxide) will be required to charge balance 0.15(Al₂O₃)—thus 0.05 K₂O+0.1CaO. These cations play no part in the depolymerization of the melt, thus A_{corr} would be derived for the composition (0.5SiO₂+0.15Al₂O₃+0.1CaO+0.1MgO) using the values tabulated above.